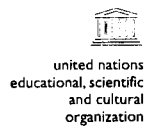


the



united nations  
educational, scientific  
and cultural  
organization

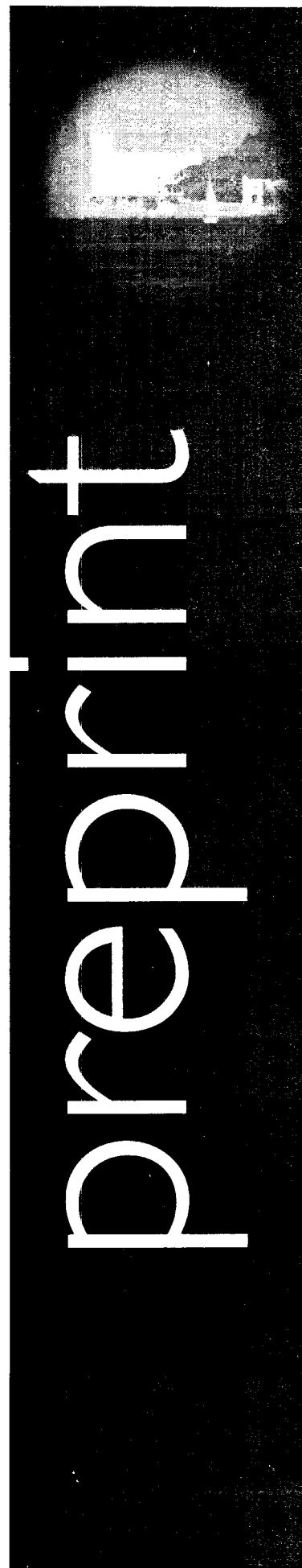


international atomic  
energy agency

**abdus salam**  
**international**  
**centre**  
**for theoretical**  
**physics**



XA0200440



Preprint

**MODELLING OF THE GROUND MOTION  
AT RUSSE SITE (NE BULGARIA)  
DUE TO THE VRANCEA EARTHQUAKES**

**Mihaela Kouteva**

**Giuliano F. Panza**

**Ivanka Paskaleva**

**and**

**Fabio Romanelli**

United Nations Educational Scientific and Cultural Organization  
and  
International Atomic Energy Agency

THE ABDUS SALAM INTERNATIONAL CENTRE FOR THEORETICAL PHYSICS

**MODELLING OF THE GROUND MOTION AT RUSSE SITE (NE BULGARIA)  
DUE TO THE VRANCEA EARTHQUAKES**

Mihaela Kouteva

*Central Laboratory for Seismic Mechanics and Earthquake Engineering,  
Bulgarian Academy of Sciences, Acad. G.Bonchev str., bl.3, Sofia, 1113, Bulgaria<sup>1</sup>  
and  
Department of Earth Sciences, University of Trieste, Trieste, 34127, Italy<sup>2</sup>,*

Giuliano F. Panza

*Department of Earth Sciences, University of Trieste, Trieste, Italy  
and  
The Abdus Salam International Centre for Theoretical Physics, SAND Group,  
Trieste, Italy.*

Ivanka Paskaleva

*Central Laboratory for Seismic Mechanics and Earthquake Engineering,  
Bulgarian Academy of Sciences, Acad. G.Bonchev str., bl.3, Sofia, 1113, Bulgaria  
and  
Fabio Romanelli*

*Department of Earth Sciences, University of Trieste, Trieste, Italy.*

MIRAMARE – TRIESTE

November 2001

---

<sup>1</sup> Permanent address.

<sup>2</sup> Present address.

## Abstract

An approach, capable of synthesising strong ground motion from a basic understanding of fault mechanism and of seismic wave propagation in the Earth, is applied to model the seismic input at a set of 25 sites along a chosen profile at Russe, NE Bulgaria, due to two intermediate-depth Vrancea events (August 30, 1986,  $M_w = 7.2$ , and May 30, 1990,  $M_w = 6.9$ ). According to our results, once a strong ground motion parameter has been selected to characterise the ground motion, it is necessary to investigate the relationships between its values and the features of the earthquake source, the path to the site and the nature of the site. Therefore, a proper seismic hazard assessment requires an appropriate parametric study to define the different ground shaking scenarios corresponding to the relevant seismogenic zones affecting the given site. Site response assessment is provided simultaneously in frequency and space domains, and thus the applied procedure differs from the traditional engineering approach that discusses the site as a single point. The applied procedure can be efficiently used to estimate the ground motion for different purposes like microzonation, urban planning, retrofitting or insurance of the built environment.

## 1. Introduction

It has been recently recognised that urban areas rather distant from earthquake sources may be prone to a seismic disaster, e.g. the earthquakes in Michoacan, Mexico'85 ( $M_w = 8.0$ ), Chilly'97 ( $M_w = 7.1$ ), Assisi, Italy'98 ( $M_w = 5.2$ ) were significantly felt within several hundred kilometres from their hypocenter. Typical examples of long periods, i.e. far-reaching, seismic effects are the ones connected with Vrancea intermediate-depth earthquakes. For example, the quake of March 4, 1977 ( $M_w = 7.5$ ), caused significant damage in Bulgaria and was felt up to Central Europe (at distances of about 1000 km).

In fact, the Vrancea seismogenic zone, situated beneath the Eastern Carpathian Arc, is one of the regional features responsible for the most destructive effects experienced in NE Bulgaria in the last years. During the last century the Bulgarian territory suffered different strong Vrancea events (e.g. 1908, 1940, 1977, 1986 and 1990) that caused significant damages at epicentral distances of several hundred kilometres. The wave field radiated by the intermediate - depth (70 to 170 km) Vrancea earthquakes, mainly at long periods ( $T > 1$  s), attenuates less with distance compared to the wave field of the earthquakes located in other seismically active zones in Bulgaria.

Through the history, more than 100 Vrancea events have been felt in Bulgaria and for 40 of them macroseismic maps were elaborated. Due to these events, intensities up to  $I = IX$  (MSK - 64) were observed at Russe, about 200 – 250 km away from Vrancea seismic sources (Rigikova, 1983) – e.g.  $I = VII$  for the Vrancea quake in 1940, and  $I = VII – VIII$  for Vrancea'77. These values match quite nicely the values that can be deduced from the recently constructed deterministic seismic hazard maps of the Circum-Pannonian region, (e.g. fig. 1-3 of Panza and Vaccary, 2000, and fig. 7 of Radualian et al, 2000, respectively), when use is made of the relation between Intensity and peak values of the seismic ground motion (Panza et al, 1999 a). The wavefield radiated by the Vrancea intermediate - depth (70 to 170 km) earthquakes, mainly at long periods ( $T > 1$  s), attenuates with distance less rapidly than the wavefield of the earthquakes in other seismically active zones in Bulgaria (Todorovska et al, 1995). Therefore the Vrancea intermediate sources should be considered as a regional danger, since large industrial areas can be seriously affected by the strong events originating in this seismogenic area. In fact, even if the Vrancea 1977 event motivated some changes in the Bulgarian Code for Design and Construction in Seismic Regions'87, the seismic excitation from 1986 and 1990 events was bigger than the prescribed seismic loading in the BG Code'87 (Paskaleva and Kouteva, 2000). The available strong ground motion database is too limited to accurately quantify the magnitude scaling and attenuation characteristics of large magnitude earthquakes (e.g. Parvez et al, 2000), and therefore the use of realistic synthetic seismograms represents a good possibility for the immediate assessment of the seismic input.

The purpose of this study is threefold:

- (1) to provide realistic synthetic signals at Russe, due to the two intermediate-depth Vrancea earthquakes of August 30, 1986 (VR86) and May 30, 1990 (VR90);
- (2) to validate these results against the available observations (Nenov et al, 1990);
- (3) using the validated modelling to quantify the site response along a representative profile crossing the town.

To simulate the ground motion at Russe, the one-dimensional (1D) modal summation technique (Panza, 1985; Panza and Suhadolc, 1987; Florsch et al, 1991; Panza et al, 2000) has been combined with the mode coupling approach (Vaccari et al, 1989; Romanelli et al, 1996, 1997). The particle motion including the inertia, body and surface forces is described by a linear system of three partial differential equations, with parameters that are dependent on the space variables. It is not possible, in general, to find an exact analytical solution for the equations describing the wave propagation in anelastic laterally heterogeneous media. In

general there are two main classes of methods to solve the equations of motion: analytical and numerical methods. Analytical methods should be preferred when dealing with models whose dimensions are several orders of magnitude larger than the representative wavelengths of the computed signal, because of the limitations in the dimensions of the model that affect the numerical techniques. Among the methods that are suitable to solve the equations of motion in flat laterally heterogeneous inelastic media with numerical techniques applied to analytical solutions, two main complementary classes can be distinguished: methods based on ray theory and methods based on mode coupling. The arrivals associated with surface waves (fundamental and higher modes) usually represent the dominant part of the seismogram and (Saragni et al, 1995) they supply the data with the most favourable signal/noise ratio for seismic hazard studies with engineering implications. Surface waves cannot be modelled easily with methods based on ray theory, because of computational problems: it is not a theoretical, but a practical limitation. On the other hand, the modal summation is a natural technique for modelling the dominant part of the seismic ground motion. The key point of the method applied is the description of the wavefield as a linear combination of given base functions: the normal modes characteristic of the medium. The technique used shares the idea that the unknown wavefield, generated by the lateral heterogeneities, can be written as a linear combination of base functions representing the normal modes (Love and Rayleigh) of the considered structure, therefore the problem reduces to the computation of the coefficients of their expansion. The basic two-dimensional (2D) model is formed by two different quarter-spaces in welded contact (fig.1).

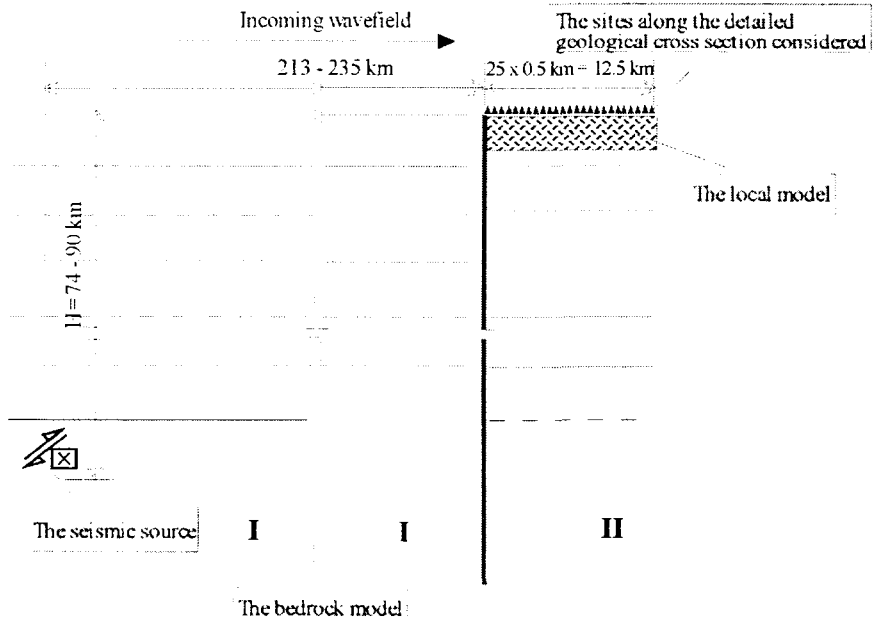


Fig. 1. Schematic description of the model adopted for the numerical experiments. The solid horizontal lines define the geological strata, the dashed lines represent the fictitious interfaces introduced to line up the layers of the two quaterspaces. The bedrock model is given in fig. 2b. The local model is given in fig. 2c. The seismic source is given in Table 1.

## 2. The Data

To construct the synthetic signals three groups of input parameters are required: (1) seismic source moment tensor, (2) geotechnical characteristics of the travelled path and (3) local site conditions. The input data used in this study consist of the seismic source moment tensor (Table 1) and of two structural models, bedrock and local structure (fig.2b, fig.2c).

The seismic source moment tensors of the Vrancea quakes of August 30, 1986 (VR86) and May 30, 1990 (VR90), as given in the CMT catalogue and that we used in the calculation, are shown in Table 1. The synthetic signals corresponding to the VR90 quake have been computed for two focal depths, 74 km and 90 km. The focal depth of 90 km corresponds to the lower limit of the depth range given by the CMT catalogue and is in agreement with some recent studies of this event (Bukchin, 2000, pers. com.).

A scheme of the relevant position of the seismic sources considered and the target site of Russe is shown in fig.2.a. In the same figure an epicentral map of the earthquakes, which occurred within the Bulgarian territory for the period 1990 - 1992, as reported in the CSEE catalogue (Shebalin et al, 1999) superimposed to the geomorphological scheme of a recently constructed seismotectonic model (Paskaleva et al, 2000) is shown.

Table 1. Seismic source parameters, CMT catalogue (Dziewonski et al, 1991)

| Earthquake identification, No/Mo/Da/Yr | Latitude [°] | Longitude [°] | Magnitude Mw | Depth [km] | Strike angle [°] | Dip angle [°] | Rake angle [°] |
|--|--------------|---------------|--------------|------------|------------------|---------------|----------------|
| 32/08/30/86 - (VR86)                   | 45.76        | 26.53         | 7.2          | -133       | 240              | 72            | 97             |
| 34/05/30/90 - (VR90)                   | 45.92        | 26.81         | 6.9          | 74 ± 16    | 236              | 63            | 101            |

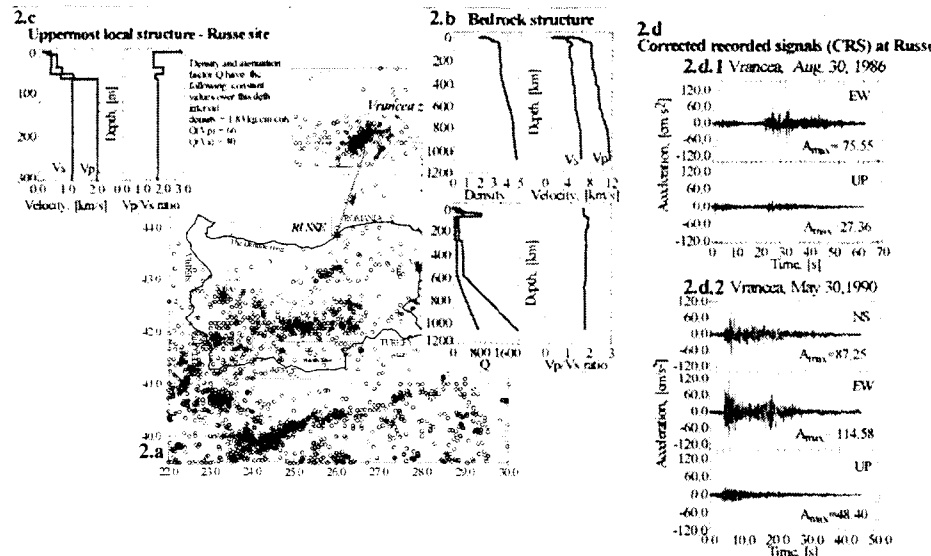


Fig. 2. THE DATA: 2.a. A scheme of the relevant position of the seismic sources considered and the target site of Russe; Epicentral map of the earthquakes, which occurred within the Bulgarian territory for the period 1990 - 1992, as reported in the CSEE catalogue (Shebalin et al. 1999), superimposed to the geomorphological scheme (poligons) of a recent seismotectonic model (Paskaleva et al, 2000); 2.b. Reference bedrock structure; 2.c. Uppermost part of the local model, below 300 m both structures have the same mechanical properties; 2.d. Corrected recorded signals (CRS) at Russe, due to Vrancea 8/30/1986 and 5/30/1990 events: NS (North - East), EW (East - West) and UP (vertical) components.

The structural information represents the average structure (bedrock) from the Vrancea seismic region to the site of Russe, and the local sedimentary layered structure of Russe site. The profile Vrancea-Russe passes through the Carpathians and the Moesian Platform, where

Pliocene and significant Quaternary deposits are present. Moving away from the Vrancea zone a gradual transition from hard rocks to unconsolidated rocks and progressively softer soils is observed. From a comparative analysis of the available structures (Paskaleva et al, 1996; Radulian et al, 1998), the structure Roma06.str (Radulian et al, 1998), shown in figure 2b, has been chosen as reference bedrock structure. The available detailed geological and geotechnical data in Russe (Evlogiev, 1993; Paskaleva et al, 1996) are used to define the uppermost part (160 m) of the local model along a cross section oriented NE 42° SW (fig. 2c). Thus, the adopted model (fig. 1) formed by two 1D models (fig. 2b and 2c) in welded contact is used in the numerical experiments.

### 3. Numerical Experiments . Discussion of the Results.

Two distinct groups of theoretical experiments have been performed. (A) Synthetic signals have been constructed and compared with the available observations, and an analysis of the influence of some reasonable variations of the seismic source moment tensor on the ground motion at the site has been done. (B) The site response along the chosen profile has been estimated and the site amplification has been mapped versus epicentral distance and frequency. All the calculations have been performed for both Vrancea earthquakes VR86 and VR90. The seismic source has been modelled with a buried double - couple. To include the free vibration periods of different types of long period construction a frequency range up to 1 Hz is considered in our computations, that are carried out independently for the P-SV and SH waves, from which transversal (TRA), radial (RAD) and vertical (VRT) components are computed. The results obtained are discussed considering acceleration time-histories  $a(t)$ , peak ground accelerations (PGA), Fourier amplitude spectra (FS) and response spectra (SA). The peak ground acceleration (PGA) is still the most common parameter, used in strong ground motion studies. In the seismic design, most frequently the acceleration response spectra, SA, are used, although there is an increasing tendency towards the use of displacements and energy spectra (e.g. Decanini and Mollaioli, 1998; Decanini et al, 1999), and for some particular analyses, the Building Codes prescribe to use the acceleration time histories,  $a(t)$ , as input for the design.

#### 3.1. *Synthetics against observations.*

The available observations in Russe are the recorded accelerograms due to the VR86 and VR90 quakes (Nenov et al, 1990). The corrected recorded signals (CRS) are shown in figure 2.d. All the records have been filtered by a low pass filter with cut-off frequency at 1 Hz, and then Fourier (FS) and response spectra, for 5% of the critical damping (SA), have been computed. Filtered corrected recorded signals (FCRS) for VR86 are shown in figure 3.1.a. Rotated non filtered CRS (RCRS) for the VR90 and rotated FCRS (RFCRS) for VR90 are shown in figures 3.2.a and 3.2.b, respectively. All the comparisons between the synthetic and the observed signals refer to the FCRS for the quake VR86 and to the RFCRS for the VR90 event.

The synthetic and observed time histories, FS and SA are compared in figures 3.1 – 3.3. In spite of the relatively simple models used for the source and for the medium, the synthetic ground motion reproduces most of the main features of the observed data. For the quake VR86, the PGA of the FCRS, (fig. 3.1.a) is larger than the synthetic one (fig. 3.1.b), but the observed and synthetic FS (fig. 3.1.c) and SA – 5 (fig. 3.1.d) are in good agreement.

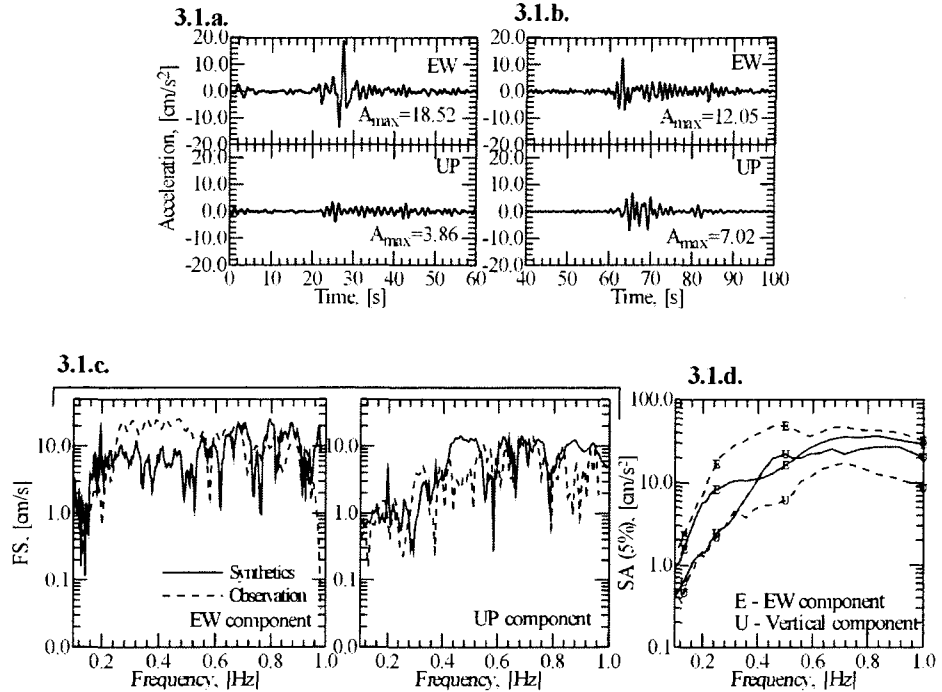


Fig. 3.1. Russe site, NE Bulgaria, Vrancea event of August 30, 1986 (VR86). Comparison between the synthetic and the observed signals. 3.1.a. The corrected recorded signal (CRS), low-pass filtered with cut-off frequency at 1 Hz; 3.1.b. Synthetic accelerogram with cut-off frequency at 1 Hz; 3.1.c. Synthetic (solid line) and observed (dashed line) Fourier spectra; 3.1.d. Synthetic (solid line) and observed (dashed line) response spectra computed for 5% critical damping (SA). East-West oriented (EW) and vertical (UP) components are shown.

The same analysis is carried out for the event VR90 (fig. 3.2). RFCRS and synthetic signals are shown in figures 3.2.b and 3.2.c, respectively. The PGA of the VRT component are practically identical, the synthetic PGA of the TRA component is about 40 % less than the observation, and the RAD component is significantly underestimated. The synthetic FS of the TRA component follows the trend of the observation, but it has lower amplitudes within the whole frequency interval considered (fig. 3.2.d). In the FS of the RAD component two distinct frequency intervals can be seen – one where the model underestimates the observation (0.2 - 0.5 Hz), and the other where there is a good agreement between the model and the observation (0.5 - 0.9 Hz), (fig. 3.2.d). The comparison between the synthetic and the observed SA is shown in figure 3.2.e, where one can see that the synthetic follow the observed spectra within the whole frequency range considered.

The comparison between the synthetic signals and the observations for the VR90, corresponding to the focal depth  $H = 90$  km used in the modelling is shown in figure 3.3. The RFCRS are shown in figure 3.3.a and the synthetic signals are shown in figure 3.3.b. A good agreement between the modelled and recorded time histories for the three ground motion components is observed (fig. 3.3.a, 3.3.b). The increment of the focal depth from 74 km (fig 3.2.c) to 90 km (fig. 3.3.c), causes an increment of  $\sim 30$  % of the PGA of TRA, of  $\sim 50$  % of the PGA of VRT, and finally of  $\sim 70$  % of the PGA of RAD. The SA amplitudes for all the three components, TRA, RAD and VRT, increase over the whole frequency range considered. The frequency content of the RAD is strongly influenced by the change of the seismic source depth (fig. 3.2.d, 3.3.d).

A comparison between VR86 (fig. 3.1) and VR90 (figs. 3.2, 3.3) shows that the PGA and SA (TRA, RAD, VRT) due to VR86 are larger than the corresponding quantities due to the VR90, both for the computed and the observed values. The same observation can be made

comparing the SA distribution versus frequency and distance for both events VR86 and VR90 – fig. 5.1.a, b and fig.5.3.a, b, respectively. This matches well with the reported macroseismic intensity, I (MSK - 64), at Russe, due to both earthquakes investigated, I = VI (VR86) and I = V (VR90) (Paskaleva et al, 2001). A further check, based on the ground velocities, obtained by integration of the seismic signals, shows a good agreement between the synthetics and observation as well. All the modelling has been made without any data fitting, but simply using the information available in the literature regarding the source, the path and the local properties. For the same events, a similar approach has led to a good agreement between the synthetics and the observed signal at Magurele, Bucharest (Moldoveanu and Panza, 1999). This is a particularly important result since the existing strong motion database is very limited, mainly for intermediate - depth strong events.

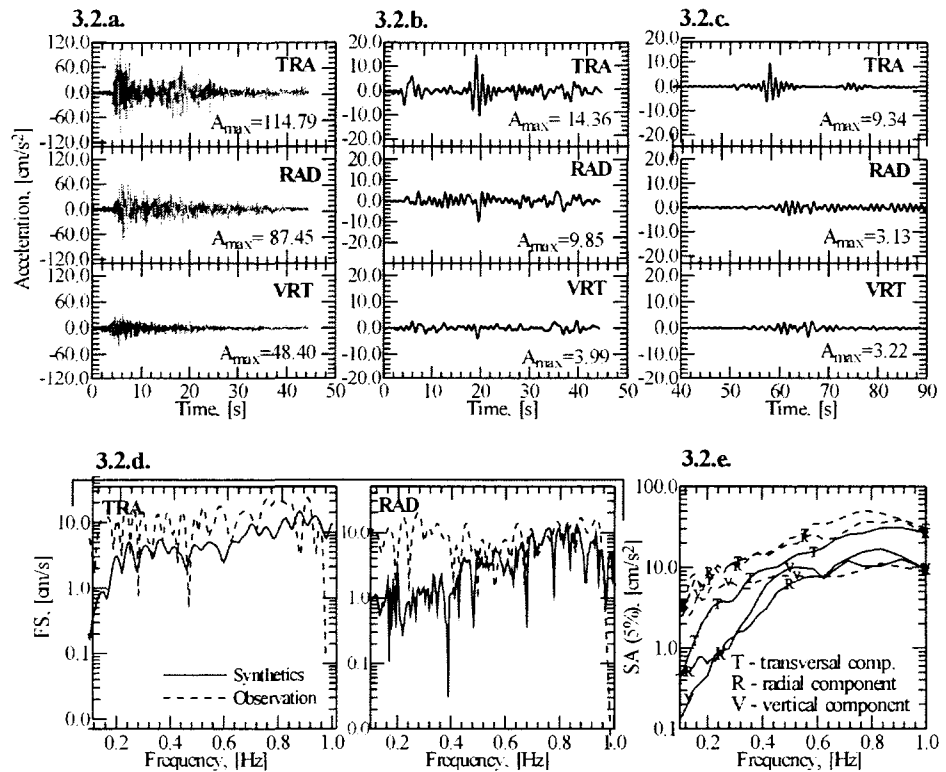


Fig. 3.2. Russe site, NE Bulgaria, Vrancea event of May 30, 1990, (VR90), focal depth  $H = 74$  km, used in the modelling. Comparison between the synthetic and the observed signals. 3.2.a. The rotated corrected recorded signal (RCRS); 3.2.b. RCRS low-pass filtered with cut-off frequency at 1 Hz; 3.2.c. Synthetic accelerogram with cut-off frequency at 1 Hz; 3.2.d. Synthetic (solid line) and observed (dashed line) Fourier spectra; 3.2.e. Synthetic (solid line) and observed (dashed line) response spectra computed for 5% critical damping (SA). Transversal (TRA), radial (RAD) and vertical (VRT) components are shown.

To test how the recorded signals are exhaustive of the possible ground amplification in Russe, some numerical experiments have been carried out varying the seismic source moment tensor and the velocity model of the uppermost 300 m of the local model, (Kouteva, 1999; Kouteva et al, 2000). Among the selected seismic source parameters, the focal depth is strongly controlling the shape and amplitude of all the components of the ground motion. Varying, within values typical for the Vrancea intermediate - depth events, the fault geometry and slip, expressed by rake, dip and strike, influences much more the RAD and VRT components than the TRA one. A change of the depth of the seismic source by 20 km (namely from 60 km to 80 km) causes changes of the PGA as large as  $\sim 50\%$  for the TRA and VRT components, and  $\sim 32\%$  for the RAD.

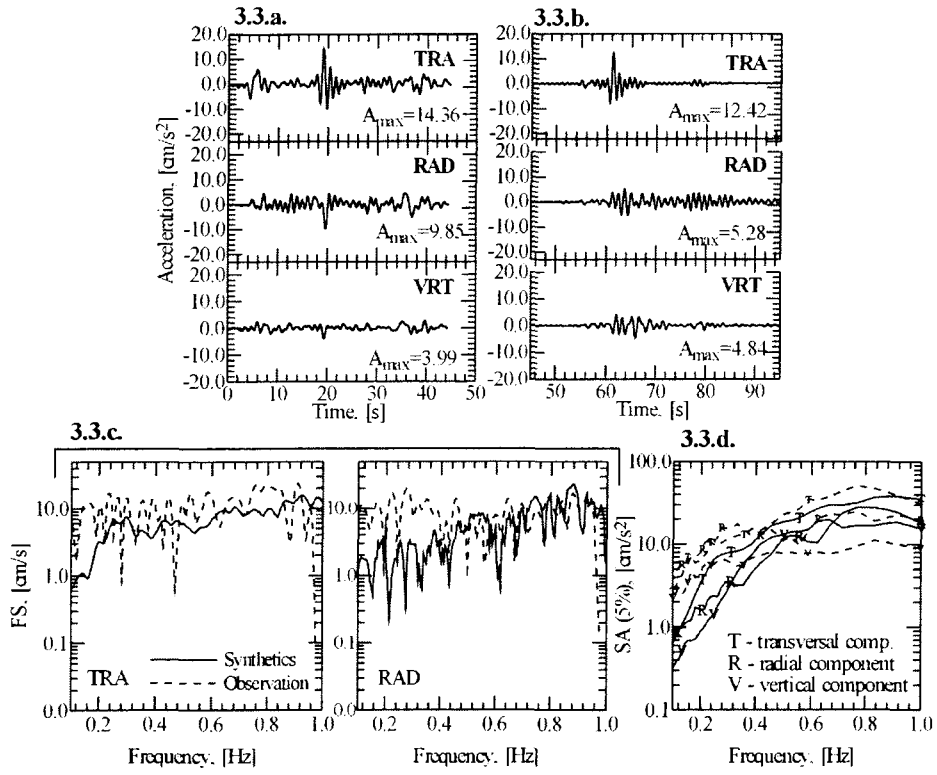


Fig. 3.3. Russe site, NE Bulgaria, Vrancea event of May 30, 1990, (VR90), focal depth  $H = 90$  km, used in the modelling. Comparison between the synthetic and the observed signals. 3.3.a. The rotated corrected recorded signal (RCRS); 3.3.b. RCRS low-pass filtered with cut-off frequency at 1 Hz; 3.3.c. Synthetic accelerogram with cut-off frequency at 1 Hz; 3.3.d. Synthetic (solid line) and observed (dashed line) Fourier spectra; 3.3.e. Synthetic (solid line) and observed (dashed line) response spectra computed for 5% critical damping (SA). Transversal (TRA), radial (RAD) and vertical (VRT) components are shown.

### 3.2. Parametric analysis of the ground motion: estimates of the influence of seismic source moment tensor variation on the ground motion at the site.

Varying the rake and strike angles, the TRA PGA changes within  $\sim 25\%$ , and it is practically not affected by the dip angle variation considered ( $\sim 5\%$ ). On the contrary, the RAD and VRT components are very sensitive to dip angle variations. If the dip angle changes by  $20^\circ$ , namely from  $53^\circ$  to  $73^\circ$ , the PGA increases by  $\sim 30\%$  for RAD and by  $\sim 50\%$  for VRT (Kouteva, 1999). Similar conclusions were reached for Magurele site, Bucharest (Moldoveanu and Panza, 1999, 2001).

Varying the geotechnical properties of the uppermost part of the local model causes obvious changes in the shape of the signals and their peak amplitudes for all of the three components (Kouteva et al, 2000). In fact, increasing the thickness of the uppermost part of the local model and the ratio  $V_p / V_s$  up to 6 for the uppermost 160 m of the 300 m (keeping  $V_s$  fixed), the PGA for all the three components increases as follows: TRA  $\sim 70\%$ , RAD  $\sim 107\%$ , VRT  $\sim 109\%$ . These results show that to obtain realistic seismic input for relatively long periods, as discussed in this study, it is necessary to consider the mechanical properties of the entire sedimentary basin characteristics. It is not enough to take into account only the uppermost 30 m or 50 m  $V_s$ , as it is assumed by the advanced today's earthquake engineering practice. The relevance of the basin depth has been recently discussed for other, more complicated, case - studies (e.g. Olsen, 2000; Joyner, 2000; Field, 2000). In agreement with our results it has been

shown that the influence of the basin depth on PGA is greater than that of detailed geology or site category (Field, 2000).

The parametric analysis (figs. 4.1 and 4.2) points out that P-SV waves (RAD) contribute significantly to the ground motion at the site, therefore all ground motion components have to be considered into the seismic input definition and not only SH waves, as it is done in common practice. The ground motion is strongly influenced by the earthquake source characteristics and, to be conservative, the hazard should be defined as the envelope of a set of different unfavourable, but credible ground motion scenarios, or as any percentage of it, depending upon the purposes. In this respect, for a single site at Russe, synthetic SA have been generated varying the seismic source moment tensor (Table 2).

In figure 4.1 (VR86), 4.2 (VR90) and Table 2 one can see the visible change of SA and its maximum value SA max, respectively, with the variation of the seismic source moment tensor for all the components, TRA, RAD and VRT. For both VR86 (fig. 4.1) and VR90 (fig.4.2) changing the strike angle, the most significant change of SA max is observed in the RAD and VRT components (VR86 ~ 26 %, VR90 ~ 28 %), while TRA changes by ~ 18 % (VR86) and ~ 16 % (VR90). The depth seems to influence both components TRA (VR86 ~ 40 %, VR90 ~ 38 %) and VRT ~ 30 %, since the RAD can differ twice for VR86 (~ 94 %) and it is practically not changed for VR90 (~ 1 %). The dip angle for both VR86 and VR90 influences mainly the RAD (VR86 ~ 125 %, VR90 ~ 47 %) and the VRT (VR86 ~ 240 %, VR90 ~ 48 %) components. The same conclusion is valid for the, RAD (VR86 ~ 240 %, VR90 ~ 68 %) and VRT (VR86 ~ 88, VR90 ~ 70 %), and TRA (VR86 ~ 4 %, VR90 ~ 8 %). The synthetic signals used to obtain the response spectra shown in figure 4.2 have been subsequently normalised to their peak values and the response spectra obtained from these normalised signals are shown in figure 4.3. To broaden the credible scenarios for the site discussed, the graphs shown in figures 4.1 and 4.2 can be expanded varying some structural parameters (e.g.  $V_p / V_s$  ratio, basin depth, Q) and an envelope curve, applicable in the engineering structural analysis, can be built up.

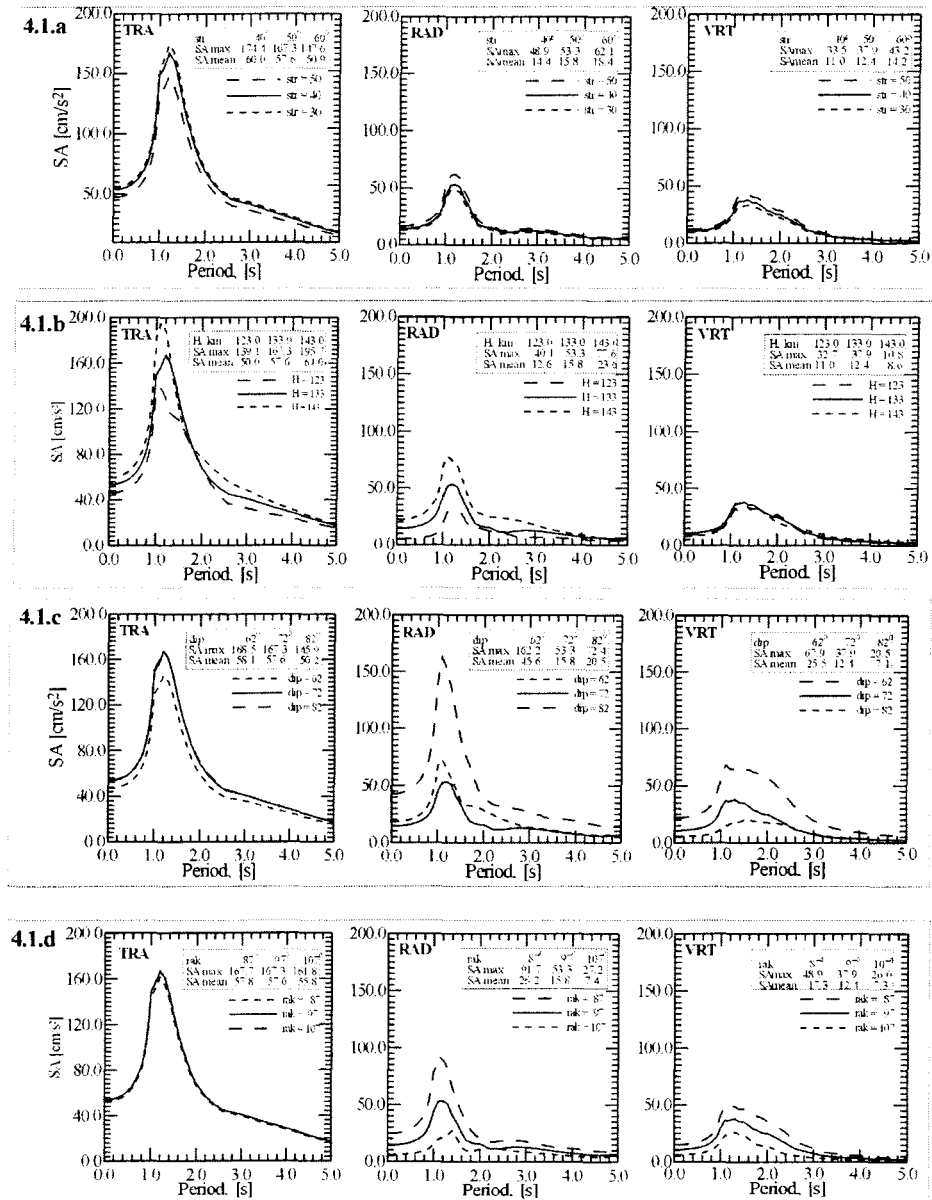


Fig. 4.1. Russe site, NE Bulgaria, Vrancea, August 30, 1986 earthquake (VR86). Variation of SA due to reasonable variation of the VR86 seismic source moment tensor, with respect to the CMT values.

4.1.a. Strike angle variation (str);

4.1.b. Focal depth variation (dpt);

4.1.c. Dip angle variation (dip);

4.1.d. Rake angle variation (rak).

Transversal (TRA), radial (RAD) and vertical (VRT) components are shown. The solid line in each graph corresponds to the CMT seismic source moment tensor, str=41°, H=133 km, dip = 63° and rak=101°.

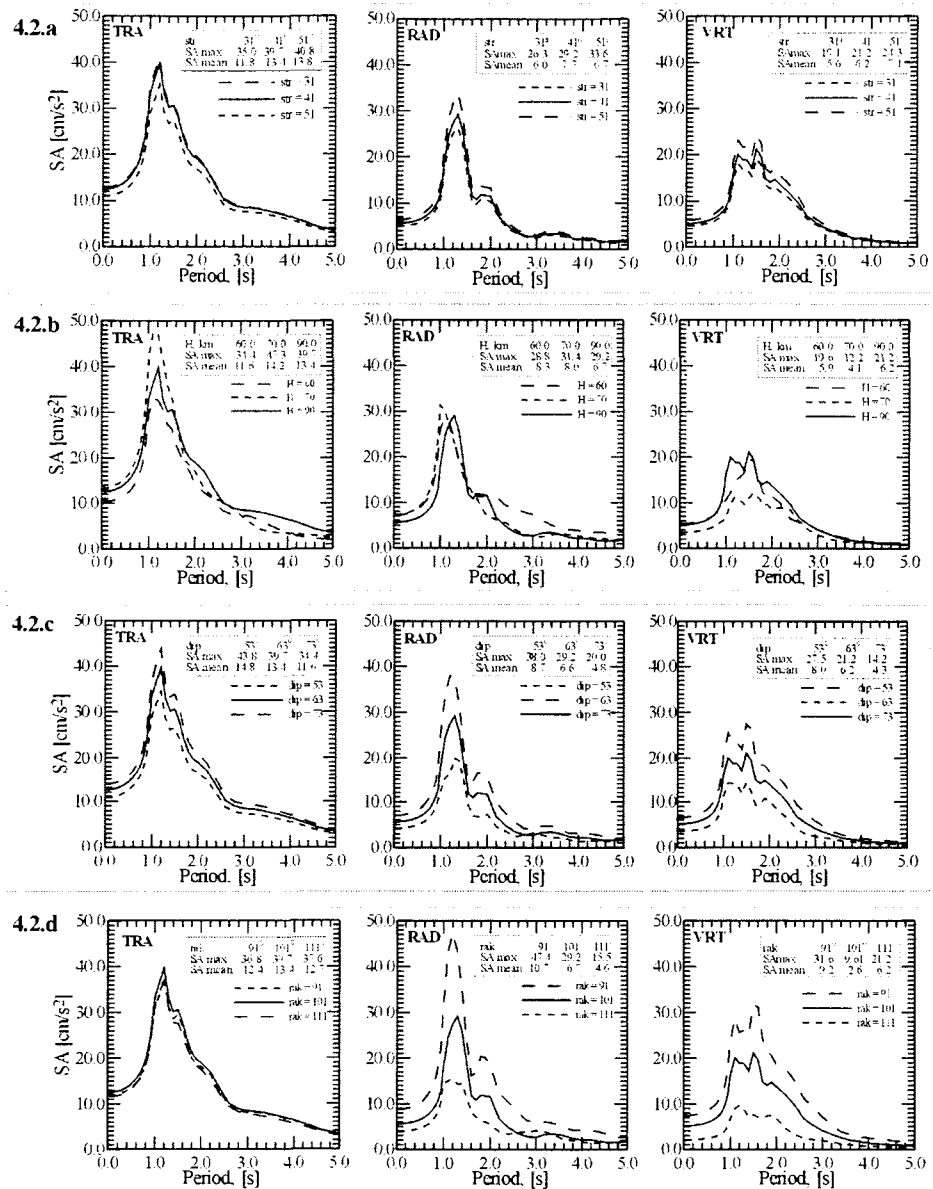


Fig. 4.2. Russe site, NE Bulgaria, Vrancea, May 30, 1990 earthquake (VR90). Variation of SA due to reasonable variation of the VR86 seismic source moment tensor, with respect to the CMT values.

4.2.a. Strike angle variation (str);

4.2.b. Focal depth variation (dpt);

4.2.c. Dip angle variation (dip);

4.2.d. Rake angle variation (rak).

Transversal (TRA), radial (RAD) and vertical (VRT) components are shown. The solid line in each graph corresponds to the CMT seismic source moment tensor, str=41°, H=133 km, dip = 63° and rak=101°.

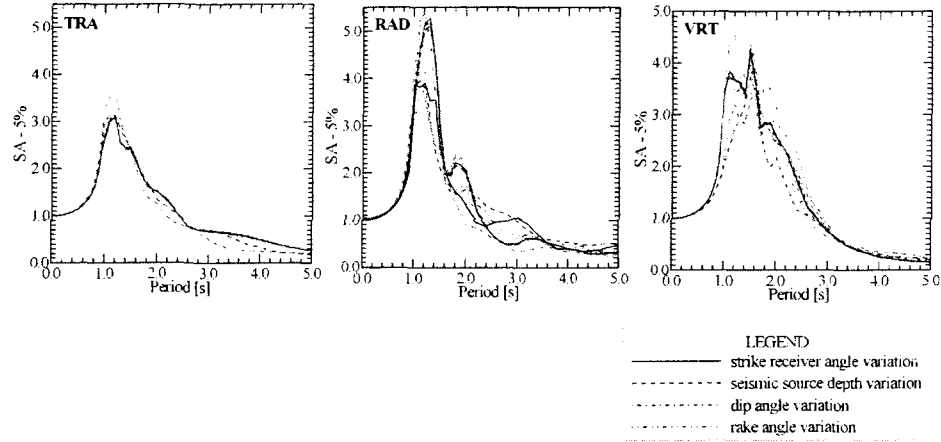


Fig. 4.3. Russe site, NE Bulgaria, Vrancea, May 30, 1990 earthquake (VR90). SA computed from the synthetic signals normalised to their peak values. Transversal (TRA), radial (RAD) and vertical (VRT) components are shown.

Table 2. Estimates of the influence of the seismic source moment tensor variation on the ground motion at a site, expressed in SA max values, calculated for different seismic source moment tensors [Strike (str), Depth (H), Dip (dip) and Rake (rak)], as shown in the table below. Comparison of the both SA computed and observed (OBS). Transverse (TRA), radial (RAD), vertical (VRT), and the horizontal East-west VR86 (EW) ground motion components are discussed.

| COMPUTED VALUES              |       |       |                                |       |       |                              |       |       |                              |       |       | OBS                                    |
|------------------------------|-------|-------|--------------------------------|-------|-------|------------------------------|-------|-------|------------------------------|-------|-------|--|
| SA max, [cm/s <sup>2</sup> ] |       |       |                                |       |       |                              |       |       |                              |       |       |  |
| <b>VR90</b>                  |       |       |                                |       |       |                              |       |       |                              |       |       | str=41,<br>H=90,<br>dip=63,<br>rak=101 |
|                              |       |       |                                |       |       |                              |       |       |                              |       |       |  |
| <i>Strike, str, [°]</i>      |       |       | <i>Depth, H, [km]</i>          |       |       | <i>Dip, dip, [°]</i>         |       |       | <i>Rake, rak, [°]</i>        |       |       |  |
| <i>H=90, dip=63, rak=101</i> |       |       | <i>str=41, dip=63, rak=101</i> |       |       | <i>str=41, H=90, rak=101</i> |       |       | <i>str=41, H=90, dip=63</i>  |       |       |  |
| 31°                          | 41°   | 51°   | 60                             | 70    | 90    | 53°                          | 63°   | 73°   | 91°                          | 101°  | 111°  |  |
| TRA                          | 35.0  | 39.7  | 40.8                           | 34.4  | 47.3  | 39.7                         | 43.8  | 39.7  | 34.4                         | 36.8  | 39.7  | 37.6                                   |
| RAD                          | 26.3  | 29.2  | 33.6                           | 28.8  | 31.4  | 29.2                         | 38.0  | 29.2  | 20.0                         | 47.4  | 29.2  | 15.5                                   |
| VRT                          | 19.1  | 21.2  | 24.3                           | 19.6  | 12.2  | 21.2                         | 27.5  | 21.2  | 14.2                         | 31.6  | 9.61  | 21.2                                   |
|                              |       |       |                                |       |       |                              |       |       |                              |       |       |  |
| <b>VR86</b>                  |       |       |                                |       |       |                              |       |       |                              |       |       |  |
|                              |       |       |                                |       |       |                              |       |       |                              |       |       |  |
| <i>Strike, str, [°]</i>      |       |       | <i>Depth, H, [km]</i>          |       |       | <i>Dip, dip, [°]</i>         |       |       | <i>Rake, rak, [°]</i>        |       |       |  |
| <i>H=133, dip=72, rak=97</i> |       |       | <i>str=50, dip=72, rak=97</i>  |       |       | <i>str=50, H=133, rak=97</i> |       |       | <i>str=50, H=133, dip=97</i> |       |       |  |
| 40°                          | 50°   | 60°   | 123                            | 133   | 143   | 62°                          | 72°   | 82°   | 87°                          | 97°   | 107°  |  |
| TRA                          | 174.4 | 167.3 | 147.6                          | 139.1 | 167.3 | 195.7                        | 168.5 | 167.3 | 146.9                        | 167.7 | 167.3 | 161.8                                  |
| RAD                          | 48.9  | 53.5  | 62.1                           | 40.1  | 53.3  | 77.6                         | 162.2 | 53.3  | 72.4                         | 91.7  | 53.3  | 27.2                                   |
| VRT                          | 33.5  | 37.9  | 43.2                           | 32.7  | 37.9  | 10.8                         | 67.9  | 37.9  | 20.5                         | 48.9  | 37.9  | 26.0                                   |
| EW                           | 27.5  | 33.7  | 62.6                           | 30.4  | 33.7  | 43.9                         | 131.5 | 33.7  | 92.5                         | 63.7  | 33.7  | 24.0                                   |

### 3.3. Site response.

Relying on the good agreement between the synthetics and the observations (fig.3 and Table 2), we have investigated the site response due to both earthquakes studied, VR86 and VR90, even if the laterally heterogeneous model is rather simple. The site response reflects the whole process of seismic waves propagation from the source to the target site including the local soil conditions (e.g. Panza et al, 1999 b) and it is really difficult to identify the different

ingredients that are controlling the resulting ground motion. The idea to reduce the uncertainties affecting the site effect determinations via waveform modelling, based on the first principals of physics, already often applied (Faeh et al, 1993; Panza et al, 2000 and references therein) is now quite widely accepted (Field, 2000).

In figures 5.1, 5.2 and 5.3 the site response due to both events VR86 (fig. 5.1) and VR90 (fig. 5.2 and 5.3) along one chosen profile at Russe is shown. The SA are obtained both for the bedrock model (fig. 5.1.a, 5.2.a, 5.3.a) and for the laterally varying one (fig. 5.1.b, 5.2.b, 5.3.b). The Response Spectra Ratios (RSR) for the TRA, RAD and VRT components are shown, as well.

From figures 5.1, 5.2 and 5.3 it is evident that both the SA and the RSR are strong functions of the source properties. Furthermore, even if the considered model is rather simple, it is possible to quantify relevant variations of the site amplification along the given local (one-dimensional) profile. These variations of the local amplifications (local soil effects) are chiefly due to the varying distance of each site from the lateral boundary. If standard methods (e.g. Lysmer et al, 1975) are applied to the considered model, all the sites would be, by definition, characterised either by the same RSR, and the resulting hazard description would be really oversimplified, if not meaningless. Thus, the approach to apply site corrections to the ground motion directly within the hazard calculations is the only sound approach as recently confirmed by other independent studies (Field, 2000). Such an approach differs significantly from the today's engineering design practice that relays upon rock - site hazard maps and applies the site correction at a later stage.

For VR86 a significant amplification of the TRA component is observed over two frequency intervals, 0.3 - 0.4 Hz and 0.7 - 0.9 Hz. The RSR for the RAD component is the most irregular in comparison with the other components, and the maximum amplification is observed at about 0.2 Hz and in the range 0.8 - 1.0 Hz (fig. 5.1.c). For VR90 ( $H = 74$  km), (fig. 5.2.3) the RSR for both horizontal components is rather irregular, and the maxima for the TRA component occur in the frequency ranges 0.2 - 0.3 Hz and 0.8 - 0.9 Hz, and for the RAD in the ranges 0.16 - 0.22 Hz and 0.7 - 1.0 Hz. For VR90 ( $H = 90$  km) (fig. 5.3) significant changes for all the three components are observed. For the TRA component (fig. 5.3.c) there are two clear peaks of the RSR, with maximum amplification in the range 0.5 - 0.8 Hz, and for the RAD component there are two frequency intervals with relatively similar amplification 0.16 - 0.20 Hz and 0.5 - 0.7 Hz. The contribution of both horizontal components to the total amplification of the ground motion in this case is not drastically different as in the previous two cases, VR86 and VR90 ( $H = 74$  km), and the RAD component is still the largest. The VRT component is characterised by visible changes in the RSR as well, but its contribution to the ground motion, in general, is very small. The results reported in figures 5.1 - 5.3 show that the RSR is quite irregular in the frequency and space domains considered. The frequency content of the synthetic signals is influenced by the focal depth and the RSR shape visibly changes going from the TRA to the RAD and VRT components (fig. 5.2.c, 5.3.c). In general, RAD is the component affected by the largest amplification, while VRT is the least affected. In common practice the contribution to seismic hazard of the RAD component, is ignored, and all the attention is routinely focused on the TRA component of motion. The result just described (fig. 5.1 - 5.3) clearly indicates how the straightforward application of common practice procedure is misleading and can lead to a severe underestimation of the hazard. Therefore, the test of the sensitivity of the site effects to the earthquake source characteristics is very important. To estimate properly the site effects, it is necessary to incorporate in the direct modelling of the wavefield all the factors controlling the ground motion at the site (Panza et al, 2000).

#### 4. Conclusions

Urban areas located at rather large distances from earthquake sources may be prone to severe earthquake hazard as well as the near field sites. The available strong ground motion database is too limited to reliably quantify the magnitude scaling and the attenuation characteristics of large magnitude earthquakes. Therefore, the use of synthetic time histories, based on a realistic modelling of the seismic source and wave propagation properties, combined with the few available pertinent records, represent a good possibility for an immediate assessment of the seismic input.

Synthetic strong ground motion records have been constructed making use of the basic principles of seismic waves propagation, considering the fault mechanism and the structural parameters of the propagation media. The direct modelling compares well with the available observations. Due to the rather simple structural lateral variations which characterise the case study, we do not think relevant the unaccounted 3D effects, for the computation of which the quantity and quality of available structural data are totally inadequate.

The results obtained show that, once a parameter has been selected to characterise the seismic ground motion, it is necessary to investigate the relationships between the values of this parameter and the properties of the earthquake source, the travelled path to the site and the geotechnical properties at the site.

This study confirms the complicated nature of the so-called “site effect”. Even in a situation with rather simple geological settings, like the one discussed in this paper, the site amplification in the frequency and space domain shows a quite irregular pattern, due to the complex interaction between the wavefield and the lateral heterogeneity. Therefore the definition of the “pure site effect” caused only by the local geological conditions, which is relying upon the convolution concept, is an oversimplification of the reality and should be replaced routinely by the estimation of the site effects via waveform modelling, based on the first principals of physics.

To obtain reliable seismic hazard assessment it is necessary an appropriate parametric study to define the different credible ground shaking scenarios, corresponding to the relevant seismogenic zones impending on a given site. To be conservative, the hazard should be defined as the envelope of these scenarios, or as a percentage of it, depending upon the purposes.

The applied procedure provides site response assessment simultaneously in the frequency and in the space domains and goes well beyond the traditional engineering approach, that discusses the site as a single point. It may be efficiently used to estimate the ground motion for the purposes of microzonation, urban planning, retrofitting or insurance of the built environment, etc.

#### Acknowledgements

This research has been performed in the framework of the UNESCO IGCP 414 Project “Realistic Modelling of Seismic Input for Mega cities and Large Urban Areas” and has been also supported by the Marie-Curie Training site grant EVK2-CT-2000-57002. All funding is gratefully acknowledged. Kind gratitude is expressed also to A. Gorshkov from MITPAN, Moscow and SAND, the Abdus Salam ICTP, for the discussion on the seismotectonic scheme of the seismogenic zones within the Bulgarian territory and to G. Leydecker from the Federal Institute for Geosciences and Natural resources, Hannover, for providing the computer file with the CSEE earthquake catalogue.

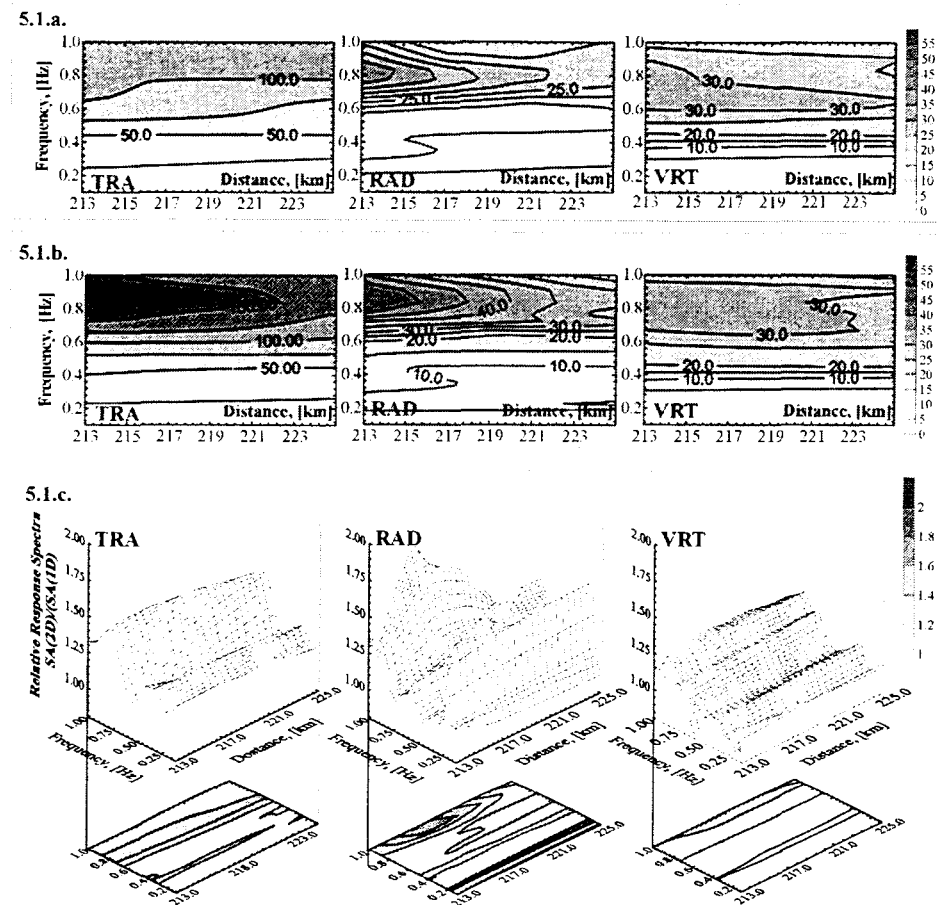


Fig. 5.1. Russe site, NE Bulgaria, Vrancea earthquake, August 30, 1986, focal depth  $H = 133$  km (VR86)

5.1.a. Distribution of SA versus frequency and distance for the bedrock model, SA (1D);

5.1.b. Distribution of SA versus frequency and distance for the laterally varying model, SA (2D);

5.1.c. Site effect: Distribution of the Response Spectra Ratio,  $RSR = SA (2D) / SA (1D)$ , versus frequency and distance.

Transversal (TRA) and radial (RAD) components are shown.

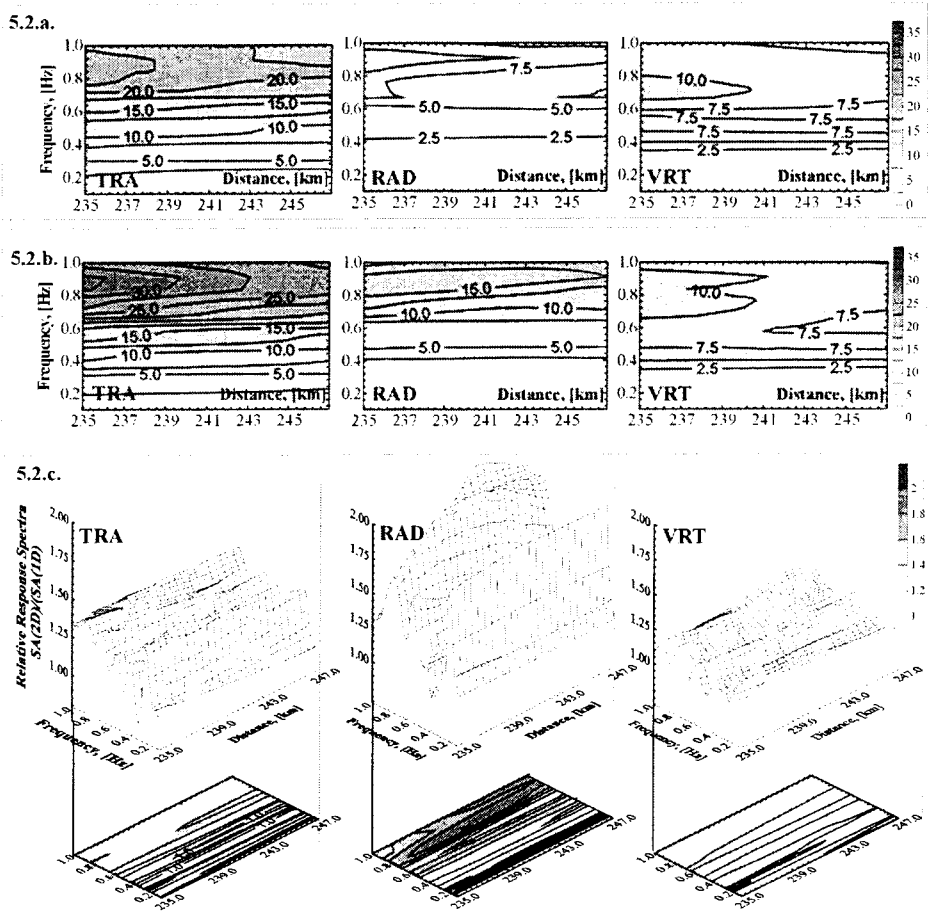


Fig. 5.2. Russe site, NE Bulgaria, Vrancea earthquake, May 30, 1990, focal depth  $H = 74$  km (VR90)  
 5.2.a. Distribution of SA versus frequency and distance for the bedrock model, SA (1D);  
 5.2.b. Distribution of SA versus frequency and distance for the laterally varying model, SA (2D);  
 5.2.c. Site effect: Distribution of the Response Spectra Ratio,  $RSR = SA (2D) / SA (1D)$ , versus frequency and distance.  
 Transversal (TRA), radial (RAD) and vertical (VRT) components are shown.

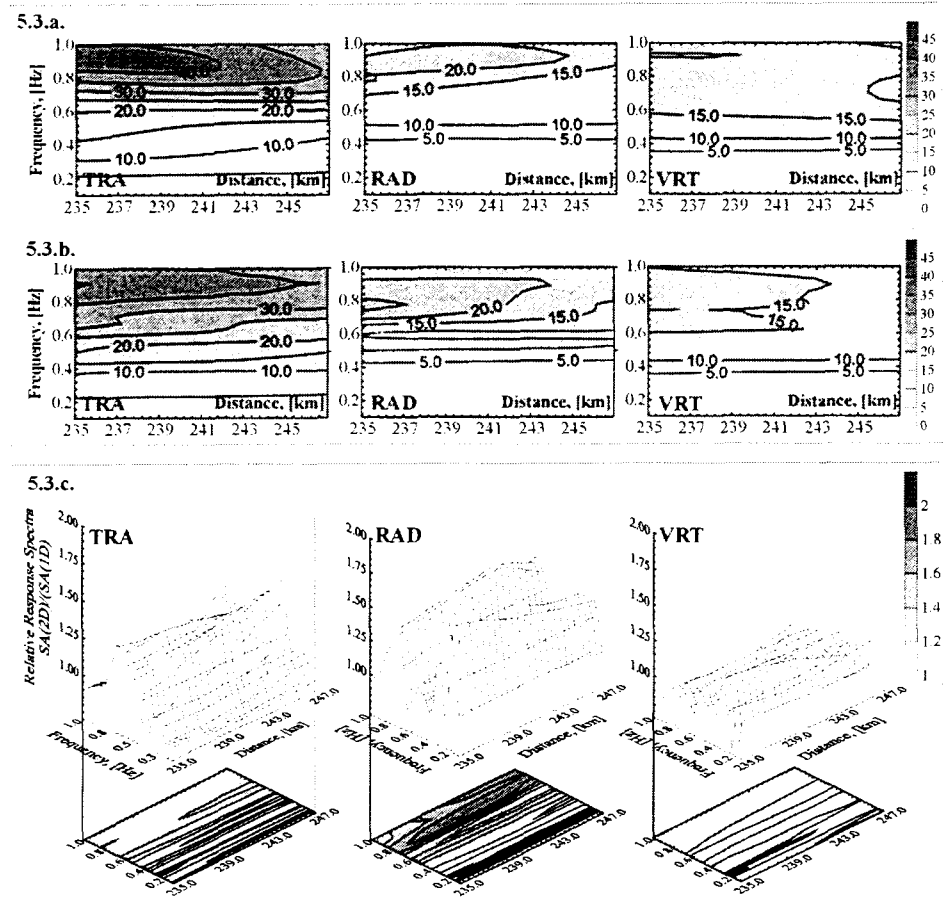


Fig. 5.3. Russe site, NE Bulgaria, Vrancea earthquake, May 30, 1990, focal depth  $H = 90$  km (VR90)  
 5.3.a. Distribution of SA versus frequency and distance for the bedrock model, SA (1D);  
 5.3.b. Distribution of SA versus frequency and distance for the laterally varying model, SA  
 (2D);  
 5.3.c. Site effect: Distribution of the Response Spectra Ratio,  $RSR = SA$  (2D) /  $SA$  (1D),  
 versus frequency and distance.  
 Transversal (TRA), radial (RAD) and vertical (VRT) components are shown.

## REFERENCES

Bukchin, B. (2000) "Activity report", the Abdus Salam ICTP – SAND group, 18p.

Decanini, L., Mollaoli, F. (1998) "Formulation of Elastic Input Energy Spectra", *Earthquake Engineering and Structural Dynamics*, 27, 1503-1522.

Decanini, L., Mollaoli, F., Panza G. F., Romanelli, F. (1999) "The realistic definition of the seismic input: application to the Catania area", in *Earthquake Resistant Engineering Structures II*, ed. G.Oliveto and Brebbia (WIT press, Boston), pp. 425-434.

Dziewonski, A. M., Ekstrom, G., Woodhouse, J. H., Zwart, G. (1991) "Centroid moment tensor solutions for April-June 1990", *Physics of the Earth and Planetary Interiors*, 66, 133-143.

Evlogiev, J. (1993) "Paleogeography and stratigraphy of the Early Pleistocene in Peridanube Northeast Bulgaria", Ph. D. thesis Geological Institute, Bulgarian Academy of Sciences, Sofia.

Faeh, D., Iodice, C., Suhadolc, P., Panza G. F. (1993) "A new method for the realistic estimation of seismic ground motion in megacities: the case of Rome", *Earthquake Spectra*, 9, 643-667.

Field, W. H. (2000) "Accounting for Site Effects in Probabilistic Seismic Hazard Analyses of Southern California", *BSSA*, 90/6/B.

Field, W., H. (2000) "A Modified Ground-Motion Attenuation Relationship for Southern California that Accounts for Detailed Site Classification and a Basin Depth Effect", *BSSA*, 90/6/B, 209-222.

Florsch, N., Faeh, D., Suhadolc, P., Panza, G. F. (1991) "Complete synthetic seismograms for high-frequency multimode SH-waves", *PAGEOPH*, 136, 529-560.

Joyner, W. B. (2000) "Strong Motion from Surface Waves in Deep Sedimentary Basins", *BSSA*, 90/6/B, 95-113.

Kouteva M. (1999) "Strong Ground Motion Modelling, Case Study of Russe, NE Bulgaria, exposed to the influence of the intermediate-depth Vrancea seismogenic zone", Final Report, East Europe Research Grant at DST, DST, University of Trieste, Trieste.

Kouteva, M., Panza G. F., Paskaleva I. (2000) "An example for ground motions in connection with Vrancea earthquakes (case study in EN Bulgaria, Russe site)", *Proc. of the 12 WCEE 2000*, Ref.2185, Auckland, New Zealand.

Lysmer, J., Uda, T., Tsai C., Seed H. B. (1975) "LUSH – a computer program for approximate 3-D analysis of soil structure interaction problems", *EERC Report No.75-30*, Earthquake Engineering Research Center, University of California, Berkeley, California, USA.

Moldoveanu, C. and Panza, G. F. (1999), "Modelling, for microzonation purposes, of the seismic ground motion in Bucharest, due to the Vrancea earthquake of May 30, 1990" in *Vrancea earthquakes: Tectonics, Hazard and Risk Mitigation*, ed. F. Wenzel, D. Lungu (Kluwer Academy Publishers), 85-97.

Moldoveanu, C. and Panza, G. F. (2001) "Vrancea Source Influence on Local Seismic Response in Bucharest", *PAGEOPH*, (in press).

Nenov, D., Georgiev G., Paskaleva I., Lee V. W., Trifunac M. D. (1990) "Strong ground motion data in EQINFO: accelerograms recorded in Bulgaria between 1981-1987" (Bulgarian Academy of Sciences, Central Lab. For Seismic Mechanics and Earthquake Engineering & Dept. of Civil engineering, University of South. California), Teprt No90-02, University of South. California, Los Angeles, California.

Olsen, K. B. (2000) Site Amplification in the Los-Angeles Basin from Three-Dimensional Modeling of Ground Motion, *BSSA*, Vol. 90/6/B, 77-95.

Panza, G. F. (1985) "Synthetic seismograms: the Rayleigh waves modal summation", *J.Geophys.*, 58, 125-145.

Panza, G. F. and Suhadolc P. (1987) "Complete strong motion synthetics", in *Seismic Strong Motion Synthetics*, ed. B. A. Bolt (Academic Press, Orlando, Computational Techniques 4), 153-204.

Panza, G.F., Vaccari, F., Cazzaro, R. (1999 a) "Deterministic seismic hazard assessment" in *Vrancea Earthquakes: Tectonics, Hazard and Risk Mitigation*, ed. F. Wenzel and D. Lungu (Kluwer Academy Publishers), 269-286.

Panza, G. F., Vaccari, F. and Romanelli, F. (1999 b) "The IUGS-UNESCO IGCP Project 414 : Realistic Modeling of Seismic Input for Megacities and Large Urban Areas. Episodes", 22, ICTP, Trieste, 26-32.

Panza, G. F., Romanelli, F., Vaccari, F. (2000) "Seismic Wave Propagation in Laterally Heterogeneous Anelastic Media: Theory and Applications to Seismic Zonation", in *Advances in Geophysics*, ed. R. Dmowska and B. Saltzman.

Panza, G. F., Radulian, M., Trifu, C. (Editors) (2000) *Seismic hazard of the Circum-Pannonian Region*, (Pageoph Topical Volumes, Birkhauser Verlag)

Panza G. F., Vaccari F. (2000) "Introduction" in *Seismic Hazard of the Circum-pannonian Region*, ed. G. F. Panza, M. Radualian and C. Trifu (Pageoph Topical Volumes, Birkhauser Verlag) pp.5-10.

Parvez I., Gusev A., Panza G.F., Petukhin A., (2000) "Preliminary determination of the interdependence among strong motion amplitude, earthquake magnitude and hypo central distance for the Himalayan region", *Geoph. J. Int.* (in press).

Paskaleva, I., Ranguelov, B., Shanov, St., Matova, M., Kouteva, M. (1996) "Intermediate NATO.ENV.LG.960916 report", DST, University of Trieste, Trieste.

Paskaleva I., Kouteva M. (2000) "An Approach for Microzonation of the Town of Russe in Connection of Recent Vrancea Earthquakes and Shabla Zone", Report on Bilateral project on Seismic Hazard and Risk Assessment of Selected Cities in the Balkan Region, DST, University of Trieste, Trieste.

Paskaleva, I., Kouteva, M., Panza, G. F., Evlogiev, J., Koleva, N., Ranguelov, B. (2001). "Deterministic approach of seismic hazard assessment in BG, Case study NE Bulgaria – the town of Russe", *Proc. of the Workshop on Deterministic Approach of Seismic Zonation of Some Balkan Countries*, Tirana, Albania.

Radulian, M., Vaccari, F., Mandrescu, N., Panza, G. F., Moldoveanu, C. L. (1998) "Seismic hazards of Romania: deterministic approach". *ICTP preprints*, IC/98/85.

Radualian M., Vaccari F., Mandrescu M., Panza G. F., Moldoveanu C. L. (2000) "Seismic hazard of Romania: Deterministic approach" in *Seismic Hazard of the Circum-pannonian Region*, ed. G. F. Panza, M. Radualian and C. Trifu, (Pageoph Topical Volumes, Birkhauser Verlag), pp. 221-248.

Rigikova, Sn. (1983) "Macroseismic maps and observations" in *Vrancea Earthquake in 1977. Its after-effects in the people's republic of Bulgaria*, ed. G. Brankov (BAS, Sofia), pp.135-150.

Romanelli, F., Bing Z., Vaccari, F. and Panza, G. F. (1996) "Analytical computation of reflection and transmission coupling coefficients for Love waves", *Geophys. J. Int.*, 125, 132-138.

Romanelli, F., Bekkevold, J. and Panza, G. F. (1997) "Analytical computation of coupling coefficients in non-poissonian media". *Geophys. J. Int.*, 129, 205-208.

Saragoni, R. G., Gomez-Bernal, A., Lobos, C. (1995) "Surface wave effect on seismic isolation: Mexico and Chile cases", *Proc. of the Int. Post-SMIRT Conference Seminar*, Santiago, Chile, pp.471-487.

Shebalin, N., Leydecker, G., Mokrushina, N. Tatevossian, R., Erteleva, O., Vassiliev, V. (1999) "Earthquake Catalogue for Central and Southeastern Europe 342 BC - 1990 AD", European Commission, Report No. ETNU CT 93 – 0087.

Todorovska, M., Paskaleva I., Glavcheva R. (1995) "Earthquake source parameters for seismic hazard assessment: examples in Bulgaria", *Proc. of the X ECCE*, Vienna, Austria.

Vaccari, F., Gregersen, S., Furlan, M. and Panza, G. F. (1989) "Synthetic seismograms in laterally heterogeneous, anelastic media by modal summation of P-SV waves", *Geophys. J. Int.*, 99, 285-295.